Journal of Medicinal Chemistry

Article

Synthesis and biological investigation of oxazole hydroxamates as highly selective histone deacetylase 6 (HDAC6) inhibitors

Johanna Senger, Jelena Melesina, Martin Marek, Christophe Romier, Ina Oehme, Olaf Witt, Wolfgang Sippl, and Manfred Jung

J. Med. Chem., **Just Accepted Manuscript** • DOI: 10.1021/acs.jmedchem.5b01493 • Publication Date (Web): 10 Dec 2015

ACS Publications

Journal of Medicinal Chemistry is published by the American Chemical Society. 1155 Sixteenth Street N.W., Washington, DC 20036

Synthesis and biological investigation of oxazole hydroxamates as highly selective histone deacetylase 6 (HDAC6) inhibitors

Johanna Senger[†], *Jelena Melesina*[‡], *Martin Marek*[§], *Christophe Romier*[§], *Ina Oehme*[⊥], *Olaf Witt*[⊥], *Wolfgang Sippl*[‡] *and Manfred Jung*[*,†]

[†]Institute of Pharmaceutical Sciences, Albert-Ludwigs-University Freiburg, Albertstraße 25, 79104 Freiburg, Germany

[‡]Institute of Pharmacy, Martin-Luther-University Halle-Wittenberg, Wolfgang-Langenbeck-Straße 4, 06120 Halle (Saale), Germany

[§]Département de Biologie Structurale Intégrative, Institut de Génétique et Biologie Moléculaire et Cellulaire (IGBMC), Université de Strasbourg (UDS), CNRS, INSERM, 1 rue Laurent Fries, 67404 Illkirch Cedex, France

[⊥]Clinical Cooperation Unit Pediatric Oncology, German Cancer Research Centre (DKFZ), Im Neuenheimer Feld 280, 69120 Heidelberg, Germany

*Corresponding author: Jung, M. (manfred.jung@pharmazie.uni-freiburg.de)

ABSTRACT. Histone deacetylase 6 (HDAC6) catalyzes the removal of an acetyl group from lysine residues of several non-histone proteins. Here we report the preparation of thiazole-, oxazole- and oxadiazole-containing biaryl hydroxamic acids by a short synthetic procedure. We identified them as selective HDAC6 inhibitors by investigating the inhibition of recombinant HDAC enzymes and the protein acetylation in cells by western blotting (tubulin vs. histone acetylation). The most active compounds exhibited nanomolar potency and high selectivity for HDAC6. For example an oxazole hydroxamate inhibits HDAC6 with an IC_{50} of 59 nM and has a selectivity index of >200 against HDAC1 and HDAC8. This is the first report showing that the nature of a heterocycle directly connected to a zinc binding group (ZBG) can be used to modulate subtype selectivity and potency for HDAC6 inhibitors to such an extent. We rationalize the high potency and selectivity of the oxazoles by molecular modelling and docking.

INTRODUCTION

Protein lysine acetylation is a reversible posttranslational modification which is balanced by histone deacetylases (HDACs) and histone acetyltransferases (HATs). Histone deacetylase 6 (HDAC6) catalyzes the cleavage of the acetyl group of ε-amino groups of lysine residues in proteins.[1] The substrates of HDAC6 are mainly non-histone substrates as tubulin[2], cortactin[3], HSP90[4] and other proteins.[5-6] HDAC6 can shuttle between cytoplasm and nucleus but is mainly localized in cytoplasm where it is associated with microtubules.[6] In nucleus it was found in protein complexes with HDAC11.[7] It consists of 1216 aa and is the only HDAC which has two functional catalytic domains[8]. Additionally there is a nuclear export signal (NES) and a serine-glutamic acid-containing tetradecapeptide (SE14) which implicate the cytoplasmic arrest and a C-terminal zinc-finger domain which binds ubiquitinated proteins.[1] With the help of this domain it is involved in the process of misfolded protein degradation and represents a promising target

for the cotreatment with proteasome inhibitors to avoid the appearance of drug resistance.[9] Additionally it is involved in many other cellular processes as cell motility, cell adhesion, cell migration, growth of cells, immune synapse formation and stress granule formation.[10] HDAC6 was found to be highly expressed in testis, as well as in liver, kidney and brain.[11] Selective inhibition of HDAC6 has arisen as a promising target for a wide range of diseases. It was shown to have influences on several kinds of neurological diseases as Alzheimer's disease[12], Huntington's disease[13-14] and Parkinson's disease[15]. Furthermore overexpression of HDAC6 is associated with the appearance of several types of cancer, solid cancers as well as hematological malignancies,[16] polycystic kidney disease[17] and other diseases.[5] As pan HDAC inhibitors often cause severe side effects, the development of selective HDAC6 inhibitors is of great interest because they are less toxic against normal cells and therefore are thought to have an improved safety profile.[11]

Several selective HDAC6 inhibitors have been reported (Chart 1).[5] Tubacin was discovered in the scope of a chemical genetics screen and was shown to inhibit cell motility.[18] Because of its high lipophilicity, it was not applicable as a drug.[5] Tubastatin A is a carbazole hydroxamic acid with an IC_{50} of 15 nM for HDAC6. It was shown to exhibit anti-hepatitis C virus activity[19] and to have neuroprotective effects without displaying the neuronal toxicity of unselective HDAC inhibitors.[18, 20] In addition it was demonstrated to have anti-inflammatory and anti-rheumatic effects.[21] Ricolinostat is a very potent but only moderately selective HDAC6 inhibitor with 10-12fold selectivity towards class I HDAC enzymes. It is part of phase I/II clinical trials in combination with dexamethasone and either bortezomib, lenalidomide or pomalidomide for the treatment of multiple myeloma.[22] A series of biaryl-[23] and pyridylalanine[24] containing hydroxamic acids was reported to inhibit HDAC6 selectively. Additionally the pyridyl

compounds showed synergistic antiproliferative effects in combination with bortezomib in breast cancer cells. Nexturastat A, a hydroxamic acid containing inhibitor with a substituted urea linker was demonstrated to exhibit low nanomolar potency on HDAC6 and very high selectivity (>600fold) towards HDAC1. It inhibited the growth of B16 melanoma cells and was shown to be the first HDAC6 inhibitor that possessed antiproliferative effects against melanoma cells.[25] ACY775 has a similar potency and selectivity profile as Tubastatin A but was shown to have a better brain bioavailability. It showed antidepressant effects which were linked to HDAC6 inhibition.[26] A common theme among many selective HDAC6 inhibitors is that they achieve their subtype selectivity by a large ring or a branched respectively Y-shaped structure and the point of branching is further away from the zinc binding hydroxamate, usually at the rim of the catalytic tunnel[25]. However, the fragment-like cyclopentenyl hydroxamate[27] also showed very good HDAC6 selectivity.

Based on initial data[28] we wanted to get insights into the structure-activity relationships (SAR) of HDAC6 inhibitors with a biaryl hydroxamate structure that do not have such a branching. Here we report that changes of the heterocycle attached to the hydroxamate have a huge impact on HDAC6 potency and selectivity and report oxazoles as such potent and selective inhibitors *in-vitro* and in cell culture.

Chart 1. Structures of selective HDAC6 inhibitors

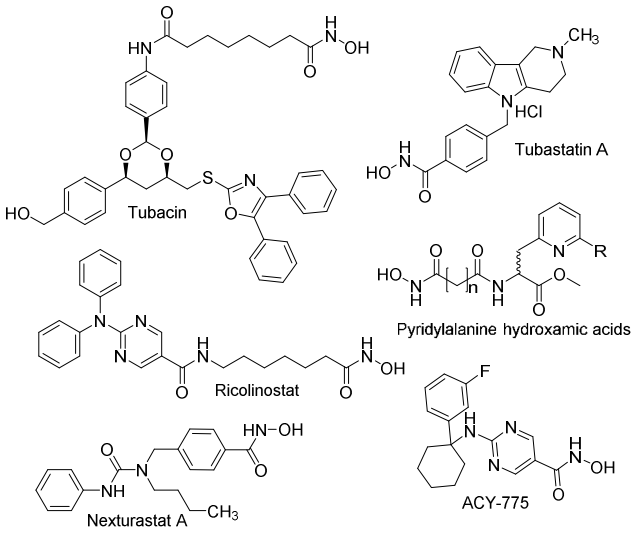

RESULTS AND DISCUSSION

2-(Pyridin-3-yl)-1,3-thiazole-4-carbohydroxamic acid (**1**) was identified by virtual screening as a selective HDAC6 inhibitor.[28] Based on this structure, we set out for structure-activity relationships to improve selectivity and inhibitory potency.

Chart 2. Lead structure (**1**)[28]

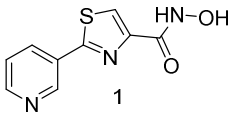

Chemistry. The first modification was the introduction of different aryl groups at the thiazole of the lead structure (Scheme 1) to get an overview on their impact on HDAC6 inhibition. The synthesis consisted of three steps: the formation of the thiazole, the cleavage of the ester and the conversion into the hydroxamic acid. In order to prepare the thiazole heterocycle, ethyl bromopyruvate and an amide were refluxed in ethanol for about 4 h. The thiazole ethylester was hydrolyzed with 1 M LiOH in THF and in the last step the carboxylic acid was activated with ethyl chloroformate and *N*-methylmorpholine to the mixed anhydride, which was converted in situ to the hydroxamic acid with hydroxylamine base. The latter was freshly prepared from hydroxylamine hydrochloride with KOH in methanol.[29]

Scheme 1. Synthesis of thiazole derivatives[a,28]

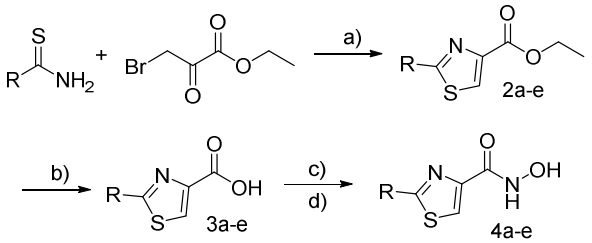

[a]Reagents and conditions: a) EtOH, 70 °C b) 1 M LiOH, THF/H_2O, RT c) $C_3H_6ClO_2$, *N*-MM, dry THF, 0 °C d) NH_2OH, MeOH, RT[29].

In a second series we then tended to the modification of the heterocycle. The synthesis of oxazoles was performed in two different ways and is described in Scheme 2. Due to the less nucleophilic oxygen the reaction had to be run under microwave irradiation and adding silver hexafluoroantimonate as a catalyst.[30] Because of the limitation to electron withdrawing amides, another synthesis strategy was performed additionally, the Suzuki coupling. The starting material consisted of a 2-bromo-oxazole and a boronic acid with different substituents. With this method it was possible to introduce a variety of different aryl groups.

Scheme 2. Synthesis of oxazole derivatives[a]

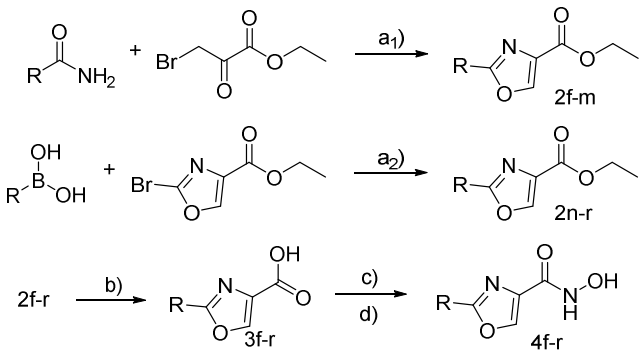

[a]Reagents and conditions: a_1) µw, $AgSbF_6$, dry DCM, 90 °C,[30] 1 h, a_2) $Pd(PPh_3)_4$, Na_2CO_3, toluene, EtOH, 120 °C, b) 1 M LiOH, THF/H_2O, RT, c) $C_3H_6ClO_2$, *N*-MM, dry THF, 0 °C, d) NH_2OH, MeOH, RT[29].

The third heterocycle that was introduced was an oxadiazole (Scheme 3). A carboxylic acid was activated to the acylchloride followed by the condensation with ethyl aminohydroxyiminoacetate[31] (**5**) and the formation of the hydroxamic acid as described above.

Scheme 3. Synthesis of oxadiazole derivatives[a]

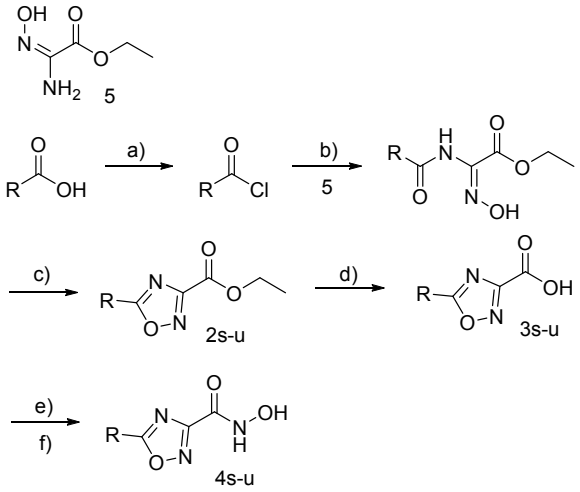

[a]Reagents and conditions: a) $SOCl_2$, 90 °C b) Et_3N, DCM c) 140 °C, DMF, 4 h[31] d) 1 M LiOH, THF/H_2O, RT e) $C_3H_6ClO_2$, *N*-MM, dry THF, 0 °C f) NH_2OH, MeOH, RT[29].

Inhibition of hHDAC1, hHDAC6 and hHDAC8. All the synthesized compounds were evaluated for their inhibitory activity against human HDAC6, HDAC1 and HDAC8 in a biochemical *In-vitro*-assay.[32] The data is summarized in Table 1. Vorinostat (SAHA)[33] was tested as a pan-HDAC reference inhibitor and cyclopentenyl hydroxamate was tested to compare the published values[27] with the ones obtained in our assay. Results are always depending on the assay and only comparable within one test system. It turned out to be 3-5 times less potent and also less selective for HDAC6 over HDAC1 when tested in our system. These outcomes indicate that our compounds are at least in our system more selective HDAC6 inhibitors in comparison to cyclopentenyl hydroxamate.

Regarding the thiazole-containing compounds **4a-e** they all showed an inhibitory effect on HDAC6 in the low micromolar region. Compared to the potency on HDAC1 and HDAC8 they were slightly more active on HDAC6. Compared to SAHA they were a bit more selective against HDAC1 but equally as or less selective against HDAC8.

In contrast, introduction of the oxazole heterocycle **4f-r** led to a huge increase in potency and selectivity. Exceptions to that trend are **4i** with a diphenylmethyl-group, **4k** with an *ortho*-substituted phenyl-residue and **4r** with a *meta*-substituted phenyl-residue that diverge from the more linear structure of the more potent analogues. They were in the inhibitory range of the thiazole compounds **4a-e** and showed approximately the same selectivity profile. All the other oxazole compounds exhibited a HDAC6 inhibition in the lower nanomolar range and showed a huge increase in selectivity towards HDAC1 and HDAC8, all of them more than 100fold. Regarding the substitution pattern of these potent and selective compounds the phenyl residue was substituted in *para*-position which seemed to be an important factor to gain selectivity. The results of compounds **4g** with a *para*-bromo-phenyl-residue and **4l, 4m** with a *para*-halogen-phenyl-residue and **4h** with a 4-biphenyl-residue are prominent examples for this. They all exhibited an IC_{50} on HDAC6 in the low nanomolar range (≤100 nM) and showed a very high selectivity towards HDAC1 and HDAC8 (from 200-400fold). There was a distinct difference between the varying heterocycles in the molecule. The thiazoles **4a-e** were much less potent and selective than the oxazole containing compounds. For the oxadiazoles **4s-u** the results were somewhat less consistent. The oxadiazole with a phenyl-residue **4s** was very potent and even more selective than the comparable oxazole compound **4f**. But in case of the oxadiazole, the increase of the aryl residue with a substitution in *para*-position did not lead to an increase but rather to loss in potency. Thus, the different factors that govern potency and selectivity don´t add in a strict additive manner.

Table 1. *In vitro* inhibition of HDAC1, HDAC6 and HDAC8

General structure: 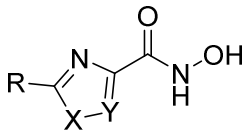								
compound	R=	X	Y	hHDAC1[a] IC_{50} [μM]	hHDAC6[a] IC_{50} [μM]	hHDAC8[a] IC_{50} [μM]	SF 6/1[b]	SF 6/8[c]
1				36% @ 10 μM[28]	0.30 [28]	n.t.	>50	-.
SAHA				0.119	0.053	1.89	2	36
Cyclopentenyl hydroxamate[27]				1.90	0.147	n.t.	13	-
				0.638[27]	0.030[27]	1.09[27]	21	363
4a		S	C	82.25	8.85	61.42	9	7
4b	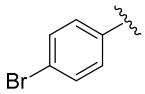	S	C	17.46	1.06	36.36	16	34
4c	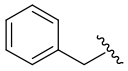	S	C	83.58	2.54	35.00	33	14
4d	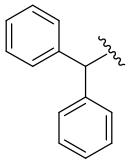	S	C	47.66	3.69	12.86	13	3
4e	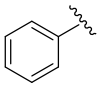	S	C	10.27	1.91	12.12	5	6
4f	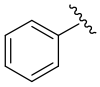	O	C	29.87	0.270	41.90	111	155
4g	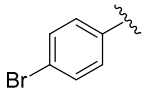	O	C	14.47	0.059	14.37	245	244

4h	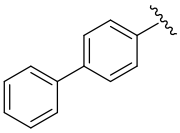	O	C	29.48	0.089	27.33	331	307
4i	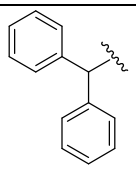	O	C	93.89	9.37	2.70	10	0.3
4j	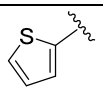	O	C	36.51	0.311	8.13	117	26
4k	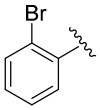	O	C	22.63	2.18	20.24	10	9
4l	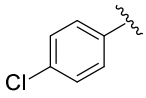	O	C	19.56	0.081	30.76	241	380
4m	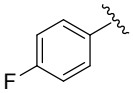	O	C	23.75	0.110	43.35	216	394
4n	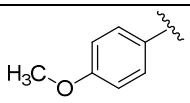	O	C	32.89	0.195	50.94	128	108
4o	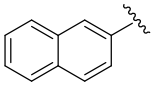	O	C	12.21	0.089	26.16	137	294
4p	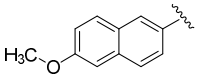	O	C	22.47	0.182	29.08	123	160
4q	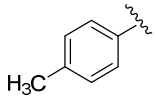	O	C	40.07	0.313	33.89	169	261
4r	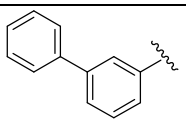	O	C	19.08	0.500	10.08	38	20
4s	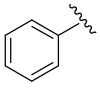	O	N	25.00	0.112	38.50	223	344

4t	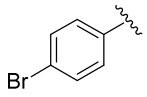	O	N	33.45	2.77	20.04	12	7
4u	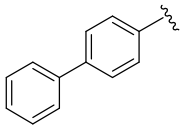	O	N	14.87	1.31	62% @ 100 μM	11	>60

[a]IC_{50} values are the means of at least two experiments. Standard deviation is <10% of the IC_{50}. [b]SF6/1: selectivity factor for HDAC6 over HDAC1 (SF6/1 = IC_{50} HDAC1/IC_{50} HDAC6), [c]SF6/8: selectivity factor for HDAC6 over HDAC8 (SF6/8 = IC_{50} HDAC8/IC_{50} HDAC6)

Ligand efficiency (LE) was determined of all the compounds for HDAC6 to evaluate the possibility for future improvement. LE is defined as the relative free binding energy in kcal/mol per number of heavy atoms (HA). It is a useful tool to predict whether the potency of a compound derives from optimal fit with the target protein or just by making many contacts.[34]

Table 2. IC_{50} values [μM] and ligand efficiencies (LE) [kcal/mol/non-H-atom] on HDAC6

Compd	**Tubastatin A**	**4a**	**4b**	**4c**	**4d**	**4e**	**4f**	**4g**	**4h**	**4i**	**4j**
HA	25	15	16	16	22	15	15	16	21	22	14
IC_{50} HDAC6	0.015[20]	8.85	1.06	2.54	3.69	1.91	0.270	0.059	0.089	9.37	0.311
LE HDAC6	0.44	0.48	0.53	0.50	0.35	0.54	0.62	0.64	0.48	0.32	0.66

Compd	**4k**	**4l**	**4m**	**4n**	**4o**	**4p**	**4q**	**4r**	**4s**	**4t**	**4u**
HA	16	16	16	17	19	21	16	21	16	17	21
IC_{50} HDAC6	2.18	0.081	0.110	0.195	0.089	0.182	0.313	0.500	0.112	2.77	1.31
LE HDAC6	0.50	0.63	0.62	0.56	0.53	0.46	0.58	0.43	0.62	0.46	0.40

Regarding the compounds with the highest ligand efficiency value, six compounds had a LE of >0.6. **4g**, **4l** and **4m** were the halogen-substituted compounds that are also very potent. Two compounds (**4f** and **4j**) are not among the most potent ones but still have high LE values because of their low molecular weight. Tubastatin A, a known selective HDAC6-inhibitor shows a LE-value of 0.44. Compared to this, several compounds had a higher LE and could therefore be further enlarged to improve their potency.

Docking study. To rationalize the inhibitory activities for HDAC1, 6 and 8 a docking study was performed. In case of HDAC1 and HDAC8 available X-ray structures were used, whereas in case of HDAC6 a homology model was generated as described in the methods part. All compounds show similar docking poses in the three target proteins: the hydroxamic acid group is coordinating the zinc ion and hydrogen-bonded to a conserved tyrosine residue (Y303 in HDAC1, Y782 in HDAC6 and Y306 in HDAC8). The thiazole, oxazole and oxadiazole linker is located in the acetyl lysine tunnel interacting with two conserved aromatic residues observed in all three HDACs (F150 and F205 in HDAC1, F620 and F680 in HDAC6, F152 and F208 in HDAC8). The nitrogen atom of the heteroaromatic ring is located nearby the conserved tyrosine of the catalytic site. The aromatic capping group is placed between a conserved aspartate and a hydrophobic residue that is different in the three isoforms (Leu271 in HDAC1, Leu749 in HDAC6, and Met272 in HDAC8). The suggested binding mode of **4b** and **4g** is shown exemplarily in Figure 1.

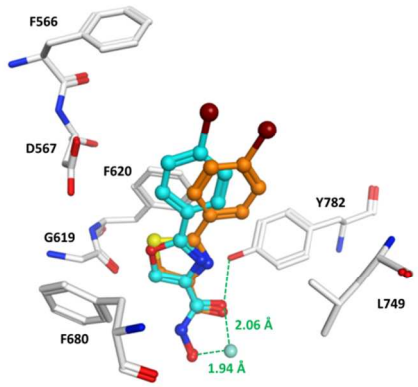

a)

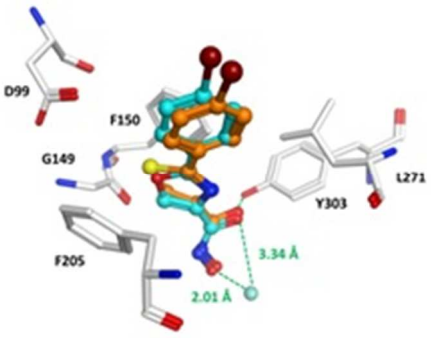

b)

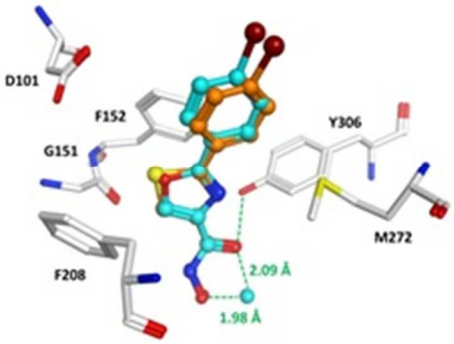

c)

Figure 1. Docking poses of HDAC inhibitors **4b** (orange) and **4g** (cyan) in HDAC6 (a), HDAC1 (b) and HDAC8 (c). The zinc ion is shown as cyan ball, Interactions between the hydroxamic acid and the zinc ion are shown as green dashed lines. Distances are given in Å.

Due to the more narrow binding tunnel observed in HDAC1 the hydroxamic acid is not able to make a perfect coordination with the zinc ion which might explain the low inhibitory activity of thiazoles, oxazoles as well as oxadiazoles (Figure 1). It has been already suggested by Butler et al. that HDAC1 has a more narrow binding tunnel than HDAC6.[20] In case of HDAC6 and HDAC8 the aromatic hydroxamic acid group is able to coordinate perfectly with the zinc ion. However, in case of HDAC8 the substituted phenyl ring is sticking out of the pocket whereas in HDAC6 the phenyl ring is interacting with residues from the loop Asp499-Pro501 that is not observed in the HDAC8 structure. In addition the shape of the HDAC6 pocket is different compared to HDAC8 mainly due to the substitution of Leu789 by Met272 in HDAC8.

To understand the selectivity of the oxazoles compared to thiazole derivatives for HDAC6 we compared the docking results of corresponding inhibitors pairs (e.g. **4b** and **4g**). Due to the more bulky sulphur in the thiazole ring and the different ring geometry the orientation of the bromophenyl ring is different for both inhibitors. In case of the oxazole the bromo (**4g**) or phenyl (**4h**) group is interacting with Phe566 and Phe520 (Figure 1a and 3) whereas in case of the thiazole (**4b**) the bromophenyl ring is not in close proximity to both residues. This might explain the high HDAC6 selectivity of *para*-substituted phenyl-oxazoles. For the oxadiazole based inhibitors similar docking poses were obtained as for the oxazoles. Here, a structural explanation for the decreased selectivity is missing. However, it should be taken into account that an interplay between two catalytic pockets of HDAC6 contributes to the final binding affinity of ligands, which makes it difficult to model these effects. Furthermore, absence of an X-ray structure of HDAC6 introduces additional uncertainty to this problem.

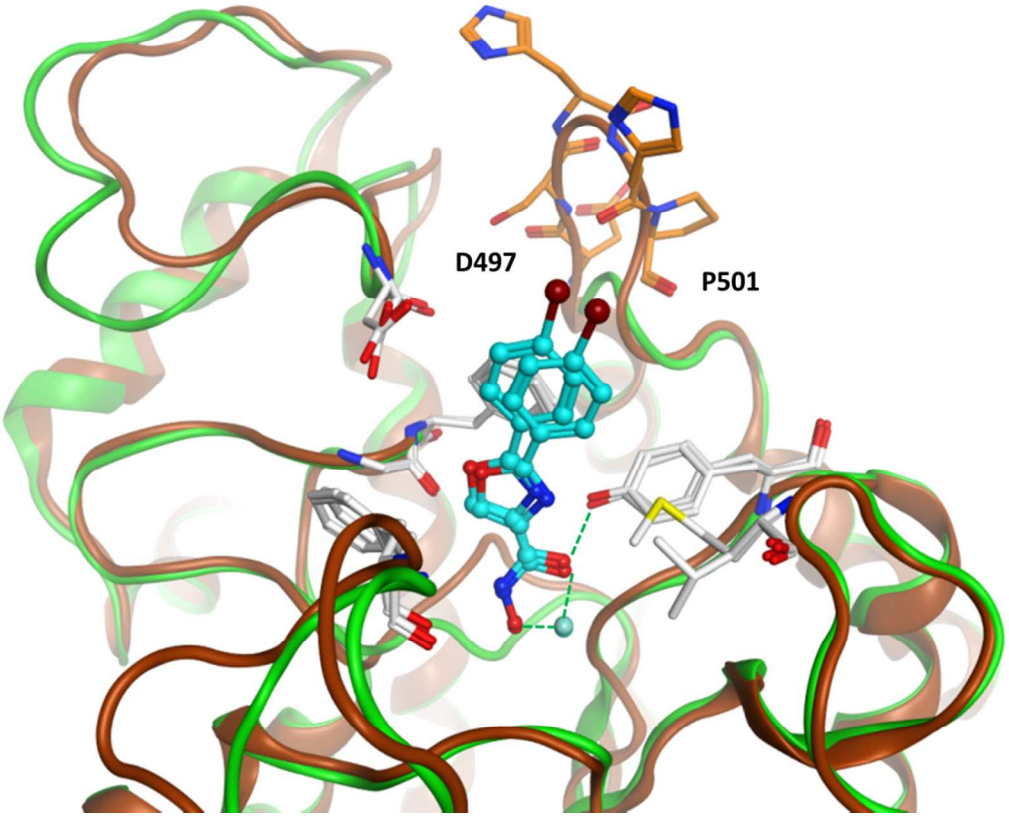

Figure 2. Comparison of HDAC6 and HDAC8 with docked inhibitor **4g** (cyan). In case of HDAC6 (brown ribbon) the bromophenyl ring of the inhibitor is stabilized by residues from an additional loop (D497-P501, shown in orange) that is not observed in HDAC8 (green ribbon).

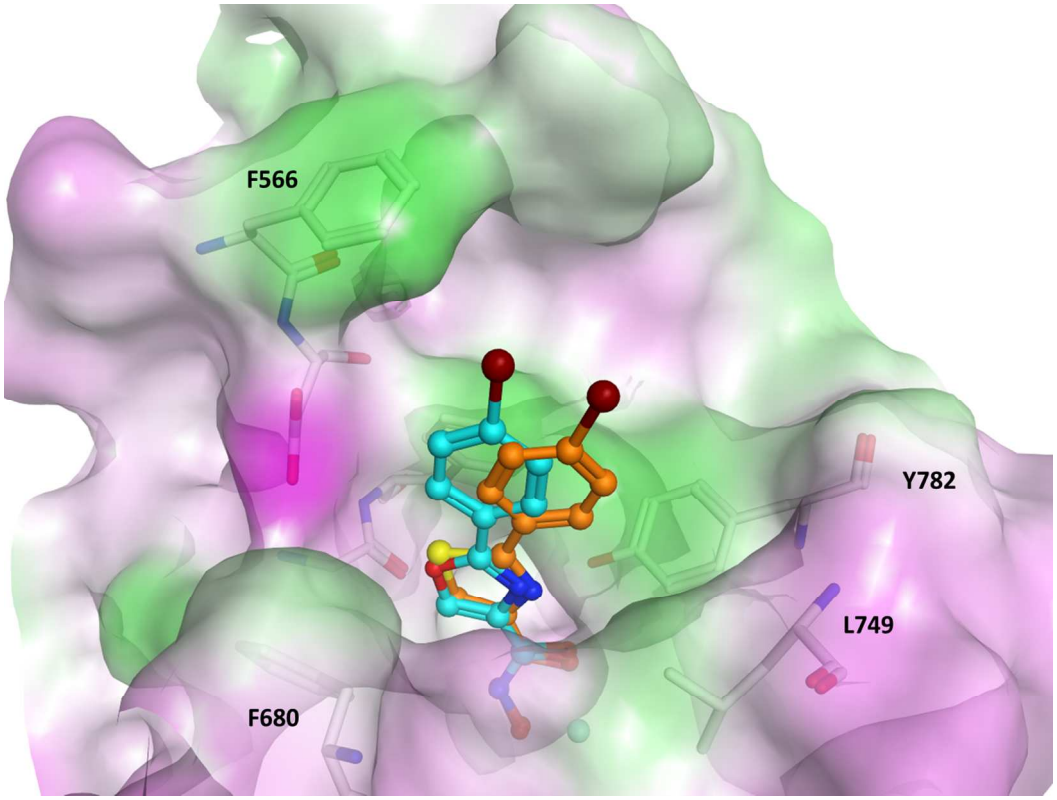

Figure 3. Molecular surface of the HDAC6 binding pocket. The orientation of two docked inhibitors, thiazole **4b** (orange) and oxazole **4g** (cyan) is shown. Only for the oxazole the phenyl ring is close to Phe520 and the bromo group in close proximity to Phe566. The surface is colored according to the lipophilicty (magenta = polar, green = hydrophobic).

Cellular data. To confirm the results obtained in the *In-vitro*-assay, western blotting experiments were performed with two of the best compounds (**4g** and **4h**) in two different cell lines. The pan-HDAC inhibitor SAHA was used as a reference compound. HeLa and HL60 cells were incubated for 4 hours with SAHA, **4g** or **4h** in three different concentrations (10 µM, 1 µM and 0.1 µM). Cell lysates were blotted against Ac-α-tubulin, Ac-histone H3 and GAPDH. As seen clearly in Figures 4 and 5 the pan-HDAC inhibitor SAHA induced both increase of tubulin acetylation and of histone acetylation in HeLa cells as well as in HL60 cells compared to DMSO

control. **4g** and **4h** in contrast only induced the acetylation of tubulin but not of histone H3 indicating that the selectivity observed in vitro is also retained in the cellular setting.

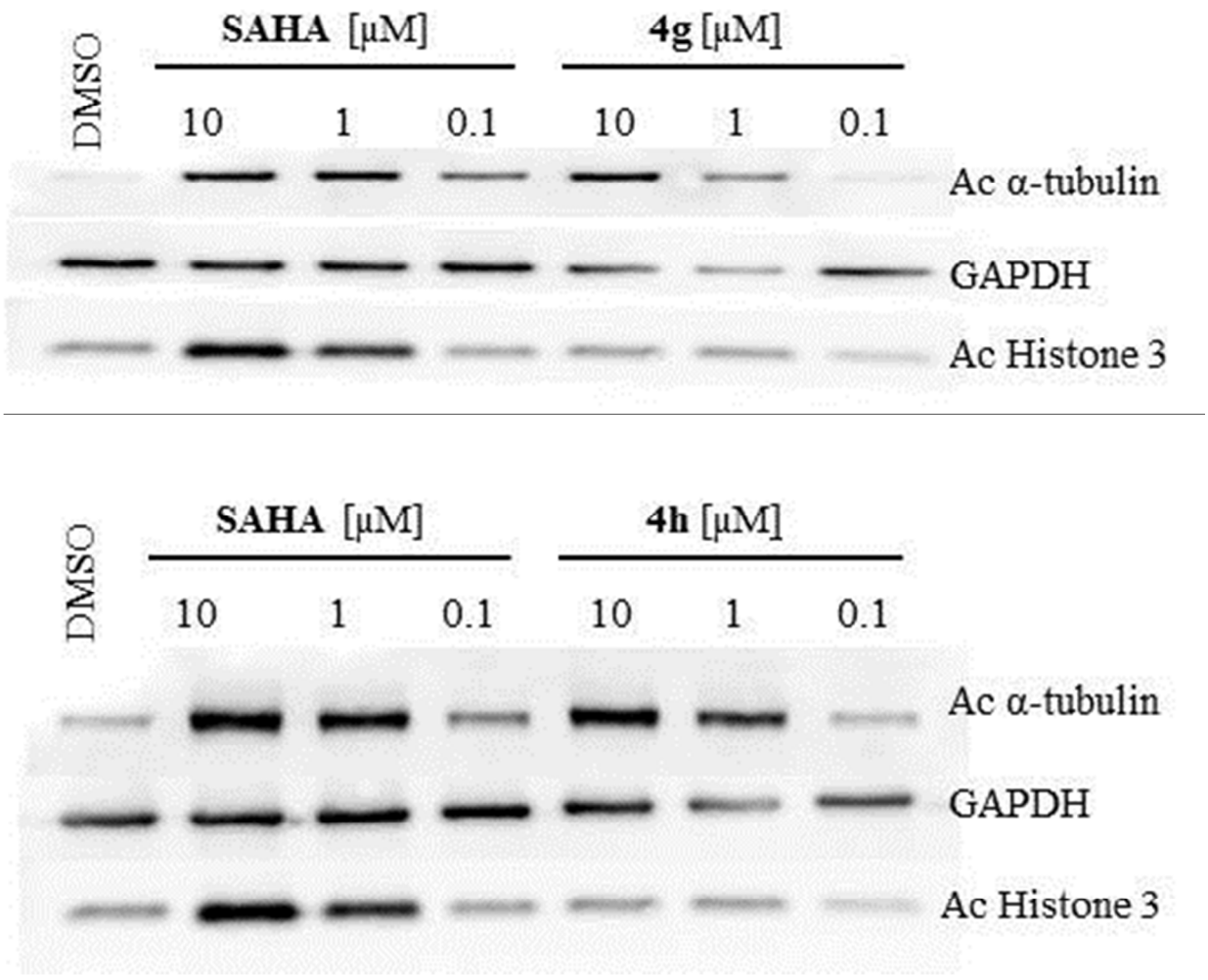

Figure 4. Western blots of acetyl-α-tubulin, acetyl-H3 and GAPDH after treatment of HeLa cells with SAHA, **4g** and **4h**. GAPDH was the loading control, DMSO the negative control.

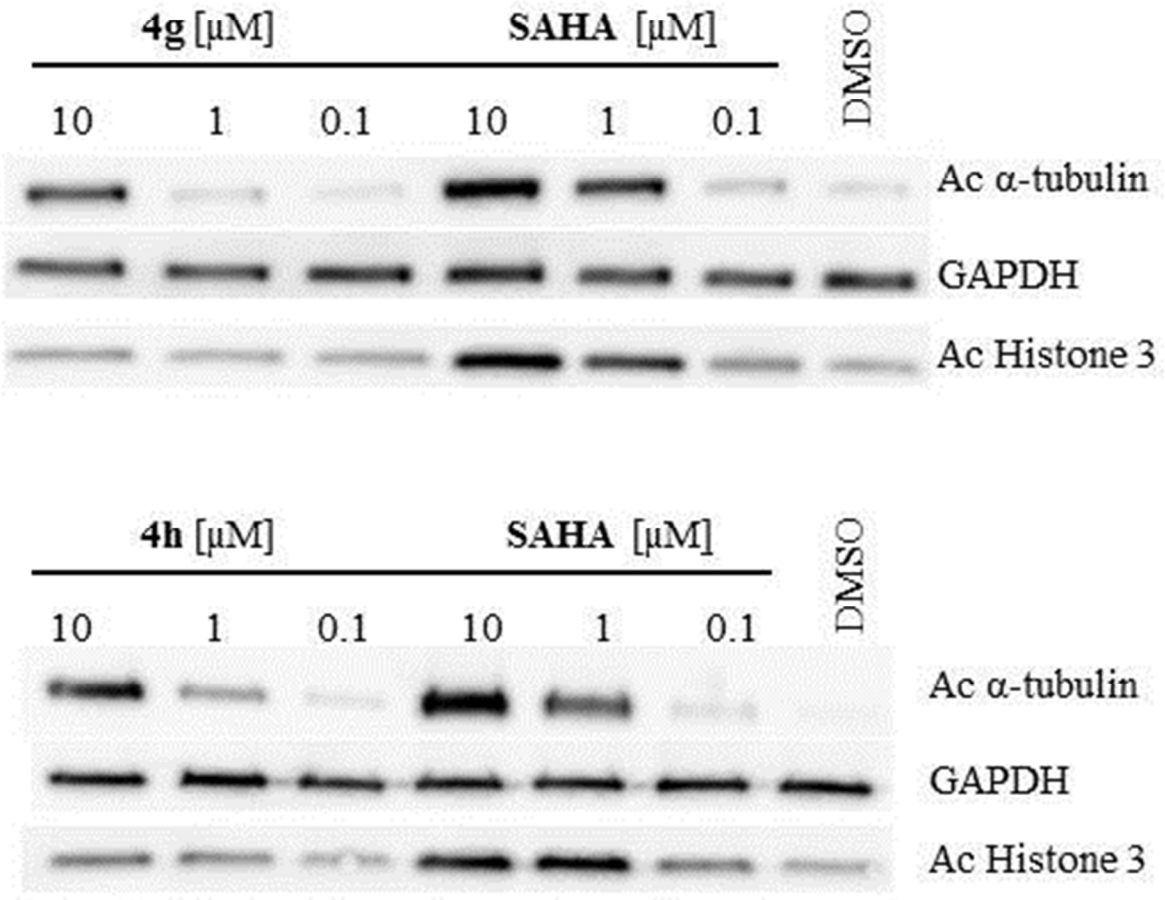

Figure 5. Western blots of acetyl-α-tubulin, acetyl-H3 and GAPDH after treatment of HL60 cells with SAHA, **4g** and **4h**. GAPDH was the loading control, DMSO the negative control.

Because of varying GAPDH levels the western blots were quantified simply by determining the ratio of acetylated tubulin versus GAPDH and of acetylated histone 3 versus GAPDH (table 3).

Table 3. Quantification of western blots in HeLa and HL60 cells

	HeLa cells (Figure 4, WB 1)			HL60 cells (Figure 5, WB 1)		
Com-pound	Ac tubulin / GAPDH	Ac H3 / GAPDH	Selectivity Index[a]	Ac tubulin / GAPDH	Ac H3 / GAPDH	Selectivity Index[a]
DMSO	1.00[b]	1.00[b]	-	1.00[b]	1.00[b]	-
SAHA 10 µM	8.99	5.86	1.53	18.36	3.50	5.25
SAHA 1 µM	9.34	3.45	2.71	14.23	2.94	4.84
SAHA 0.1 µM	3.61	0.77	4.69	2.59	1.77	1.46
4g 10 µM	16.03	1.76	9.11	12.39	1.32	9.39
4g 1 µM	16.13	4.34	3.72	1.52	1.14	1.33
4g 0.1 µM	0.96	0.56	1.71	0.84	1.11	0.76
	HeLa cells (Figure 4, WB 2)			HL60 cells (Figure 5, WB 2)		
DMSO	1.00[a]	1.00[a]	-	1.00[a]	1.00[a]	-
SAHA 10 µM	6.89	3.79	1.82	97.38	4.83	20.16
SAHA 1 µM	5.10	2.01	2.54	51.53	5.39	9.56
SAHA 0.1 µM	1.89	0.59	3.20	5.49	1.94	2.83
4h 10 µM	7.03	0.83	8.47	61.01	2.10	29.05
4h 1 µM	8.99	1.61	5.58	13.56	1.46	9.29
4h 0.1 µM	1.56	0.51	3.06	3.53	1.11	3.18

[a]Selectivity index defined as quotient of Ac Tub/GAPDH divided by Ac H3/GAPDH. [b]All values have been normalized to DMSO.

It can be seen that **4g** and **4h** induced the acetylation of tubulin at concentrations of 10 µM and 1 µM to a greater extent as compared to the acetylation of histone H3. In comparison to SAHA the accumulation of acetylated tubulin versus acetylated histone H3 is more pronounced, especially at the higher concentrations. This indicated and confirmed the HDAC6 selectivity of these compounds also on a cellular level.

Similar results were obtained with western blot experiments in the neuroblastoma cell line BE(2)-C. Cell lysates of **4b** and **4g** were blotted against acetyl-tubulin, acetyl-histone H4 and actin as a loading control (see Figure S1). It could be clearly seen that the acetylation of tubulin with 10 µM of **4g** was induced stronger than the acetylation with 10 µM of **4b**.

This confirmed the results obtained in the *in-vitro* testing where activity and selectivity of the oxazole **4g** was clearly superior to the thiazole **4b**. To analyze the antiproliferative effects of these compounds the CellTiter 96 AQ_{ueous} Non-Radioactive Cell Proliferation Assay (Promega) was performed on HL60 cells with compounds **SAHA**, **4b, 4f, 4g, 4h, 4m, 4n** and **4o** (Table 4). It was shown before that HDAC6 plays a role as a target for antileukemic drugs in acute myeloid leukemia.[35] SAHA as a pan HDAC inhibitor is very effective with a GI_{50} of 80 nM. All the other compounds showed an antiproliferative effect on HL60 cells in the micromolar range. The four most effective compounds were 4h with a GI_{50} of 5.60 µM, **4o** with a GI_{50} of 6.30 µM, **4b** with a GI_{50} of 11.06 µM and **4g** with 10.22 µM.

Table 4. Antiproliferative effects on HL60 cells determined with the CellTiter 96 AQ_{ueous} Non-Radioactive Cell Proliferation Assay (Promega)

compound	**GI_{50} [µM]**[a]
SAHA	0.08
4b	11.06
4f	44.06
4g	10.22
4h	5.60
4m	30.10
4n	29.23
4o	6.30

[a]GI_{50} values are the means of at least two experiments. Standard deviation is <10% of the GI_{50}. Experiments were performed in triplicates.

Additionally, the cell proliferation assay was performed on HeLa cells with compound **4g**. The GI_{50} value of **4g** was determined with a value of 23.69 µM. Compared to the reference substance SAHA with a value of 1.68 µM, the selective HDAC6 inhibitor seemed to be less toxic in HeLa cells.

It is difficult to dissect whether antiproliferative potency is caused by selective HDAC6 inhibition or residual class I HDAC inhibition. Several compounds showed an *in-vitro* efficacy on HDAC6 similar to SAHA but the antiproliferative effects on HL60 cells were less pronounced with selective HDAC6 compounds compared to pan-HDAC inhibitors as SAHA. This may additionally be confounded by differences in cellular uptake or stability. The i*n-vitro* selectivity was additionally confirmed in two different cell lines with western blot experiments with clearly visible effects at concentrations of 10 µM and 1 µM.

CONCLUSION

Based on **1**, found by virtual screening, we explored a new biaryl HDAC6 inhibitor scaffold with three different heterocycles attached to the hydroxamate. We demonstrated that oxazole-containing inhibitors showed the best activity and selectivity for HDAC6 compared to thiazole- and oxadiazole-containing ones. The variation of the aryl-substituent attached to the heterocycle indicated that in order to gain the best selectivity and potency results, the phenyl-group should be substituted at 4-position with a halogen- or another phenyl-ring. Substitution in *ortho*- or *meta*-position had a diminishing effect on potency and selectivity on HDAC6. All the synthesized molecules showed HDAC6 inhibition and selectivity *in vitro*. The most potent and selective compounds were **4g**, **4h** and **4o**. We also confirmed the HDAC6 selectivity of **4g** and **4h** in cell culture with western blotting of tubulin versus histone acetylation. Several compounds were tested for their antiproliferative activity on HL60 cells and showed effects in the low micromolar range. Thus, this is the first example that just the exchange of the heteroatom from sulfur to oxygen in the aryl ring adjacent to the zinc binding modules is sufficient to modulate the activity towards very high HDAC6 potency and selectivity. The good ligand efficiency shows that these compounds can be optimized further, probably by attaching the common branched substitution patterns further outwards from the zinc ion.

EXPERIMENTAL SECTION

Chemistry. All reagents were obtained from commercial sources and used without further purification. ^{1}H-NMR and ^{13}C-NMR spectra were recorded on Bruker Avance DRX spectrometer at 400 MHz and 100 MHz. Chemical shifts were reported in parts per million (ppm, δ) with TMS as internal standard. Compounds were dissolved in DMSO-d_6 or in D_3COD. Standard abbreviations indicating multiplicity were used as follows: s = singlet, bs = broad singlet, d = doublet, t = triplet, q = quartet and m = multiplet. Aromatic ^{1}H-NMR proton signals were generally described as multiplets. Thin-layer chromatography (TLC) was performed using Merck 60 F_{254} silica gel plates. All yields were not optimized. Flash chromatography was performed using Isolera One (Biotage) with a linear solvent gradient.

A purity of >95% for all the final compounds was determined with HPLC (Agilent 1260 Infinity, Agilent) and UV detection at 210 nm. Elution was performed under gradient conditions: Eluent A: H_2O containing 0.05% TFA, Eluent B: acetonitrile (MeCN) containing 0.05% TFA. Linear gradient conditions were as follows: 0–4 min, A = 90%, B = 10%; 4–29 min, linear increase to 100% of B; 29–31 min, B = 100%; 31–40 min, A = 10%, B = 90%. Method 1 (M1), analytical column, Phenomenex Synergi 4 µm MAX-RP 80 Å, 150 x 4.6 mm, flow rate 1 mL/min. Method 2 (M2), analytical column, Phenomenex Synergi 4 µm POLAR-RP 80 Å, 150 x 4.6 mm, flow rate 1 mL/min. Method 3 (M3), analytical column, Phenomenex Synergi 4 µm HYDRO-RP 80 Å, 250 x 4.6 mm, flow rate 1 mL/min.

Mass spectra were recorded with a TSQ700 from Thermo Fisher using APCI (NH_3) or ESI. Melting ranges were determined in glass capillary tubes with the Stuart Melting Point Apparatus SMP2.

Infrared spectra were recorded with a Spectrum Two™ FT-IR Spectrometer with a diamond

universal ATR sampling accessory from PerkinElmer and analysed with the Spectrum 10™ software.

Method A. **General synthesis of ethyl aryl-1,3-thiazole-4-carboxylates (2a-e).** Thioamide (1 equiv) and ethyl bromopyruvate (1.2 equiv) were dissolved in ethanol and heated to 70 °C. The reaction was monitored with TLC until completion. The solvent was evaporated and the ethylester (2a-e) was purified by flash column chromatography (ethyl acetate : cyclohexane 3:7 (V/V)).

Ethyl 2-(pyrazin-2-yl)-1,3-thiazole-4-carboxylate (2a). 557 mg (4 mmol) pyrazine-2-thiocarboxamide and 602 µL (4.8 mmol) ethyl bromopyruvate were used according to method A. ^{1}H-NMR (DMSO-d_6, δ [ppm]): 9.33-9.32 (m, 1H, 3'-H), 8.80-8.79 (m, 1H, 5'-H), 8.75-8.74 (m, 1H, 6'-H), 8.71 (s, 1H, 5-H), 4.38-4.33 (q, 2H, O-C$\underline{H_2}$-CH_3, ^3J = 7.1 Hz), 1.36-1.32 (t, 3H, O-CH_2-C$\underline{H_3}$, ^3J = 7.1 Hz). ^{13}C-NMR: (δ [ppm]): 166.9 (2-C), 160.9 (C=O), 148.1 (4-C), 146.7 (5'-C), 145.6 (2'-C), 145.0 (6'-C), 141.0 (3'-C), 132.4 (5-C), 61.5 (O-$\underline{C}H_2$-CH_3), 14.6 (O-CH_2-$\underline{C}H_3$)

Method B. General synthesis of aryl-1,3-thiazole-4-carboxylic acids (3a-e). The ethylester (**2a-e**) was hydrolysed by dissolving it in THF/H_2O, adding 1 M LiOH (4 equiv) and stirring at RT for 0.5-4 hours controlled by TLC. Upon completion of the reaction the solvent was evaporated in vacuum and the reaction mixture was extracted with ethyl acetate. The aqueous layer was acidified with 2 M HCl to pH 4 until the product precipitated. The suspension was extracted with ethyl acetate three more times. The combined organic layers were dried over Na_2SO_4 and evaporated in vacuum obtaining the carboxylic acids (**3a-e**).

2-(pyrazin-2-yl)-1,3-thiazole-4-carboxylic acid (3a). 371 mg (1.6 mmol) **2a** and 6.3 mL (6.3 mmol) LiOH (1 M) were used according to method B. ^{1}H-NMR (DMSO-d_6, δ [ppm]): 13.30 (bs,

1H, COOH), 9.33 (m, 1H, 3'-H), 8.81-8.80 (m, 1H, 5'-H), 8.76-8.75 (m, 1H, 6'-H), 8.67 (s, 1H, 5-H). ^{13}C-NMR: (δ [ppm]): 166.6 (2-C), 162.3 (COOH), 149.3 (4-C), 146.8 (5'-C), 145.7 (2'-C), 145.0 (6'-C), 141.1 (3'-C), 132.0 (5-C).

Method C. General synthesis of aryl-1,3-thiazole-4-carbohydroxamic acids (4a-e). The carboxylic acid (**3a-e**) was dissolved in THF under nitrogen atmosphere and activated by adding ethyl chloroformate (1.2-1.5 equiv) and *N*-methylmorpholine (1.3-1.5 equiv) at 0 °C. After stirring the reaction for 10 min, the precipitated salts were filtered off. Hydroxylamine was freshly prepared by stirring hydroxylamine hydrochloride (1.5-20 equiv) and potassium hydroxide (1.5-20 equiv) in methanol at 0 °C for 15 minutes and filtering off the resulting potassium chloride. The two filtrates were combined and stirred for 30 minutes at room temperature. Afterwards the solvent was evaporated and the reaction mixture was purified by flash column chromatography (dichloromethane : methanol = 95:5 (V/V)) and crystallisation or by preparative reversed phase chromatography (acetonitrile : water = 45:55 (V/V))

2-(pyrazin-2-yl)-1,3-thiazole-4-carbohydroxamic acid (4a). 91 mg (0.4 mmol) **3a**, 51 µL (0.53 mmol) ethyl chloroformate, 63 µL, (0.6 mmol) *N*-methylmorpholine, 46 mg (0.7 mmol) hydroxylamine hydrochloride and 37 mg (0.7 mmol) potassium hydroxide were used according to method C. Overall yield : 85 mg (10%). Mp: 179-181 °C. ^{1}H-NMR (DMSO-d_6, δ [ppm]): 11.42 (bs, 1H, NH-OH), 9.49 (m, 1H, 3'-H), 9.30 (bs, 1H, NH-OH), 8.79-8.78 (m, 1H, 5'-H), 8.74-8.73 (m, 1H, 6'-H), 8.45 (s, 1H, 5-H). ^{13}C-NMR: (δ [ppm]): 166.2 (2-C), 158.4 (CONH), 150.2 (4-C), 146.6 (5'-C), 145.9 (2'-C), 144.5 (6'-C), 141.7 (3'-C), 126.8 (5-C). MS (APCI, m/z): 223.0283 $[M + H]^+$. Purity >99% (10.98 min, M3).

Method D and E: General synthesis of Ethyl aryl-1,3-oxazole-4-carboxylates.

Method D (2f-n): Amide (1 equiv), ethyl bromopyruvate (1.2-1.5 equiv) and silver hexafluoroantimonate (1 equiv) were mixed in dry methylene chloride in a 15 mL microwave tube. The tube was sealed and put in the microwave for one hour at 30 watt, 5 bar and 90 °C. Afterwards, saturated $NaHCO_3$ solution was added and the reaction mixture was extracted with ethyl acetate. The combined organic layers were washed with brine, dried over Na_2SO_4 and the solvent was evaporated off in vacuum. The product was purified by flash column chromatography (ethyl acetate : cyclohexane 3:7 (V/V)). Hydrolysis of the ester (**3f-n**) and formation of the hydroxamic acid (**4f-n**) was performed as described in methods B and C.

Ethyl 2-phenyl-1,3-oxazole-4-carboxylate (2f). 827 g (6.8 mmol) benzamide, 1.0 mL (8.2 mmol) ethyl bromopyruvate and 2.3 g (6.8 mmol) silver hexafluoroantimonate were used according to method D. ^{1}H-NMR (DMSO-d_6, δ [ppm]): 8.95 (s, 1H, 5-H), 8.04-8.01 (m, 2H, 2'-,6'-H), 7.59-7.57 (m, 3H, 3'-,4'-,5'-H), 4.35-4.30 (q, 2H, O-C$\underline{H_2}$-CH_3, ^3J = 7.1 Hz), 1.33-1.30 (t, 3H, O-CH_2-C$\underline{H_3}$, ^3J = 7.1 Hz). ^{13}C-NMR (δ [ppm]): 161.7 (2-C), 161.1 (C=O), 146.1 (5-C), 134.1 (4-C), 131.8 (4'-C), 129.7 (3'-,5'-C), 126.7 (2'-,6'-C), 126.4 (1'-C), 61.1 (O-$\underline{C}H_2$-CH_3), 14.6 (O-CH_2-$\underline{C}H_3$).

Method E (2o-r): Suzuki-coupling. $Pd(PPh_3)_4$ (0.1 equiv) was dissolved in 5 mL/mmol toluene and stirred together with ethyl 2-bromo-1,3-oxazole-4-carboxylate (1 equiv) in a round bottom flask. The aryl-boronic acid (1.5 equiv) was dissolved in 5 mL/mmol EtOH and added to the mixture. Finally, aqueous Na_2CO_3 solution 2 M (10 equiv) was added. After heating the mixture to 120 °C for 2-5 hours 50 mL methylene chloride were added and the organic layer was separated, dried over Na_2SO_4 and evaporated. The product was purified by flash column chromatography (ethyl acetate : cyclohexane 3:7 (V/V)). Hydrolysis of the ester (**3o-r**) and formation of the hydroxamic acid (**4o-r**) was performed as described in method B and C.

Ethyl 2-(naphthalene-2-yl)-1,3-oxazole-4-carboxylate (2o). 225 mg (1.0 mmol) ethyl 2-bromo-1,3-oxazole-4-carboxylate, 264 mg (1.5 mmol) 2-naphthyl-boronic acid, 118 mg (0.1 mmol) $Pd(P(Ph)_3)_4$ and 5.1 mL (10.0 mmol) Na_2CO_3 (2 M) were used according to method E. ^{1}H-NMR (DMSO-d_6, δ [ppm]): 8.95 (s, 1H, 5-H), 8.63 (m, 1H, 1'-H), 8.12-8.11 (m, 1H, Ar-H), 8.09-8.08 (m, 2H, Ar-H), 8.01-7.98 (m, 1H, Ar-H), 7.64-7.61 (m, 2H, Ar-H), 4.36-4.30 (q, 2H, O-C$\underline{H}_2$-CH_3, ^3J = 7.1 Hz), 1.34-1.30 (t, 3H, O-CH_2-C$\underline{H}_3$, ^3J = 7.1 Hz). ^{13}C-NMR (δ [ppm]): 161.9 (C=OOEt), 161.3 (2-C), 146.2 (5-C), 134.3 (4-C), 134.3 (Ar-C), 132.9 (Ar-C), 129.5 (Ar-C), 129.2 (C-Ar-H), 128.4 (Ar-C), 128.2 (Ar-C), 127.6 (Ar-C), 127.0 (1'-C), 123.7 (2'-C), 123.3 (3'-C), 61.2 (O-$\underline{C}H_2$-CH_3), 14.6 (O-CH_2-$\underline{C}H_3$).

Method F: General synthesis of ethyl aryl-1,2,4-oxadiazole-3-carboxylates (2s-u). Thionyl chloride (3 mmol) was added dropwise to the carboxylic acid (1 equiv) in dry methylene chloride. After completion of the addition the mixture was heated to 90 °C for 2-3 hours. Remaining thionyl chloride and solvent were removed with a stream of nitrogen. The acyl chloride was directly processed further by adding ethyl 2-oximinooxamate (1 equiv) and dissolving it in methylene chloride (5 mL) at 0 °C. Triethylamine (1.5 equiv) was added dropwise. The reaction mixture was stirred for 1 to 3 hours. After completion (TLC-control) the solvent was evaporated and dimethylformamide (2-3 mL) was added to the reaction. The mixture was heated to 150 °C until completion (TLC-control) of the formation of the oxadiazole. After completion the mixture was extracted with ethyl acetate and washed with water. The product was purified by flash column chromatography (ethyl acetate : cyclohexane 3:7 (V/V)). Hydrolysis of the ester (**3s-u**) and formation of the hydroxamic acid (**4s-u**) was performed as described in method B and C.

Ethyl 5-phenyl-1,2,4-oxadiazole-3-carboxylate (2s). 485 mg (4.0 mmol) benzoic acid, 864 µL (12.0 mmol) thionyl chloride, 525 mg (4.0 mmol) ethyl 2-oximinooxamate and 825 µL (6.0 mmol) triethylamine were used according to method F. ^{1}H-NMR (DMSO-d_6, δ [ppm]): 8.18-8.16 (m, 2H, 2'-,6'-H), 7.78-7.74 (m, 1H, 4'-H), 7.69-7.64 (m, 2H, 3'-,5'-H), 4.48-4.42 (q, 2H, O-C$\underline{H_2}$-CH_3, ^{3}J = 7.1 Hz), 1.38-1.34 (t, 3H, O-CH_2-C$\underline{H_3}$, ^{3}J = 7.1 Hz). ^{13}C-NMR (δ [ppm]): 176.9 (5-C), 162.5 (C=OEt), 157.6 (3-C), 134.3 (4'-C), 130.1 (3'-,5'-C), 128.5 (2'-,6'-C), 123.2 (1'-C), 63.0 (O-$\underline{C}H_2$-CH_3), 14.3 (O-CH_2-$\underline{C}H_3$).

***In-vitro*-testing**[32]. OptiPlate-96 black microplates (Perkin Elmer) were used. Assay volume was 60 µL. 52 µL of human recombinant HDAC1 (BPS Bioscience, Catalog #: 50051) or human recombinant HDAC6 (BPS Bioscience, Catalog #: 50006) in incubation buffer (50 mM Tris–HCl, pH 8.0, 137 mM NaCl, 2.7 mM KCl, 1 mM $MgCl_2$ and 1 mg/mL BSA) were incubated with 3 µL of different concentrations of inhibitors in DMSO and 5 µL of the fluorogenic substrate ZMAL (Z-(Ac)Lys-AMC)[36] (126 µM) for 90 min at 37 °C. After incubation time 60 µL of the stop solution, comprising 33 µM Trichostatin A (TSA) and 6 mg/mL trypsin in trypsin buffer (Tris–HCl 50 mM, pH 8.0, NaCl 100 mM), were added. The plate was incubated again at 37 °C for 30 min and fluorescence was measured on a BMG LABTECH POLARstar OPTIMA plate reader (BMG Labtechnologies, Germany) with an excitation wavelength of 390 nm and an emission wavelength of 460 nm.

Inhibition of human HDAC8 was measured in ½ AREAPLATE-96 F microplates (Perkin Elmer) with an assay volume of 30 µL. HDAC8 enzyme was obtained as described before.[37] 22.5 µL of enzyme in incubation buffer (50 mM KH_2PO_4, 15 mM Tris, pH 7.5, 3 mM $MgSO_4$*7 H_2O, 10 mM $MgSO_4$) were mixed with 2.5 µL of inhibitor in DMSO and 5 µL of Z-L-Lys(ε-trifluoroacetyl)-AMC (150 µM). The plate was incubated at 37 °C for 90 min. 30 µL of the stop

solution (see HDAC1 and HDAC6) were added and the plate was incubated again at 37 °C for 30 min. Measurement was performed as described for HDAC1/6.

Cell culture. HeLa cells (ATCC CCL-2) were cultured in Dulbecco's modified Eagle's medium (DMEM, 4.5 g/l glucose) containing 10% FBS Gold, 2 mM L-glutamine, 100 U/ml Penicillin and 100 µg/mL Streptomycin. 0.8*10^5 cells per well were seeded in a six-well plate overnight and then incubated with different concentrations of compounds for 4 hours. Cells were washed with PBS, lysed in 100 µL SDS Sample Buffer (Cell signaling, 62.5 mM Tris-HCl (pH 6.8 at 25 °C), 2% w/v SDS, 10% v/v glycerol, 50 mM dithiothreitol, 0.01% bromophenol blue) and harvested by scraping them off the plate and transferring them to an eppendorf tube. After sonicating for 5-10 min, to shear DNA and reduce sample viscosity, the samples were heated to 95 °C for 1 minute. Cell extracts were used directly for SDS-PAGE or kept frozen at -20 °C until usage.

For the SDS-PAGE 15 µL of cell extracts were loaded onto a 12.5% SDS-gel and run at 160 V followed by the transfer to a nitrocellulose membrane via western blotting for antibody-based detection.

After transfer the non-specific binding was blocked by incubating the membrane in 25 mL blocking buffer (5% non-fat dry milk in Tris-Buffered Saline with 0.1% Tween 20 (TBS-T)) for 1 hour at room temperature or at 4 °C overnight. After washing the membrane 3 times for 5 minutes with TBS-T, the primary antibody (anti-acetylated α-tubulin (Sigma Aldrich, 1:1000)) was added in 3% milk in TBS-T for 3 h at room temperature or overnight at 4 °C. Before exposing the membrane with the secondary antibody it was washed again three times for 5 min with TBS-T to remove unbound primary antibody. The secondary antibody anti-mouse-IgG-HRP (Sigma Aldrich, 1:10000) was added in 3% milk in TBS-T at room temperature for 1 hour.

Afterwards the membrane was washed again. The detection was performed via enhanced chemiluminescence (ECL Prime) after incubation for 5 minutes in the dark with a FUSION-SL (PEQLAB) and the FUSION-CAPT software. After detection of acetylated tubulin the whole procedure was repeated with the primary antibody anti-acetyl-Histone H3 (Millipore, 1:2000) and the secondary antibody anti-rabbit IgG-HRP (Sigma Aldrich, 1:10000) to detect the acetylation of Histone H3 and again with the primary antibody anti-GAPDH (Sigma Aldrich, 1:5000) and the secondary antibody anti-rabbit IgG-HRP (Sigma Aldrich, 1:10000) to control the loading amount.

CellTiter 96 AQ_{ueous} Non-Radioactive Cell Proliferation Assay (Promega). HL60 cells (ATCC CCL-240) were plated in 96-well plates at a density of 5000 cells per well in RPMI supplemented with 10% fetal bovine serum, 2 mM L-glutamine, 100 U/ml Penicillin and 100 µg/mL Streptomycin. The final culture volume was 100 µL. Cells were treated with 0.05% DMSO as a control or with various concentrations of inhibitors.

HeLa cells were plated in 96-well plates at a density of 2000 cells per well and allowed to adhere overnight in DMEM supplemented with 10% fetal bovine serum, 2 mM L-glutamine, 100 U/ml Penicillin and 100 µg/mL Streptomycin. Next day, the cells were treated with 0.1% DMSO as a control or with various concentrations of inhibitors.

Cell proliferation was determined by using the Celltiter 96 Aqueous nonradioactive cell proliferation assay (Promega, Madison WI). The 3-(4,5-dimethylthiazol-2-yl)-5-(3-carboxymethoxyphenyl)-2-(4-sulfophenyl)-2H-tetrazolium/phenazine methosulfate (MTS/PMS) solution was mixed at a ratio of 20:1, and 20 µL were added per well to 100 µL of culture medium after an incubation time of 72 hours. GI_{50} values are the means of at least two experiments. Standard deviation is <10% of the GI_{50}. Experiments were performed in triplicates.

After 72 h the plates were measured at 490 nm absorbance after 2-4 h using a multiwell-plate spectrophotometer. The background was determined by measuring the absorption of cell culture medium and MTS-PMS in the absence of cells and was subtracted from all values. GI_{50} was defined as the concentration that led to 50% viable cell number.

Ligand efficiency. Ligand efficiency (LE, Δg) values were calculated as illustrated by Hopkins et al.[34] LE is defined as the ratio of free energy binding to the number of heavy atoms ($\Delta g = \Delta G/N_{HA}$). It is described that IC_{50} values from percentage inhibition can be substituted for K_d-value. The free energy of ligand binding was calculated as follows: $\Delta G = -R*T*\ln(IC_{50})$ with $R = 1.987*10^{-3}$ kcal/K/mol and T = 310 K.

Computational methods. Since the HDAC6 X-ray structure is not available, a homology model of this protein has been generated. Amino acid sequence of HDAC6 was retrieved from the Uniprot database[38] (Q9UBN7) and used as a search query in the Protein Data Bank[39] to identify candidate template structures with BLAST[40] algorithm. Despite the higher similarity score to class IIa HDACs (HDAC4 and HDAC7), the crystal structure of HDAC8 (PDB ID 1T69) has been chosen as the template, because it contains the catalytically important tyrosine residue (Y306). Also it is known that inhibitors of HDAC8 often inhibit HDAC6 too. The amino acid sequence of HDAC6 shows that it contains two HDACs catalytic domains, but only the second catalytic domain of HDAC6 was modeled for simplicity. The amino acid sequence alignment was performed with CLUSTAL O 1.2.0[41] and used to generate a homology model of HDAC6 with the program MODELLER 9.11[42].

Protein models of HDAC1 (PDB ID 5BKX), HDAC6 (homology model) and HDAC8 (PDB ID 2V5X) were prepared for docking using Protein Preparation Wizard (Schrödinger Inc.)[43]. Missing hydrogen atoms were added to the structures, the protonation states of the residues were

assigned and a small minimization with the RMSD deviation shortcut of 0.3 Å was run to relax the protein. Ligand structures were prepared from smiles and subjected to conformational search in MOE 2012.10 within an energy window 5 kcal/mol[44] to produce unbiased low-energy starting conformations for docking. Molecular docking experiments were performed using Glide (Schrödinger Inc.)[43]. GlideSP score was used to rank the docking poses. Figures were prepared in MOE 2012.10.

ASSOCIATED CONTENT

Supporting information. Additional experimental details and spectral data for the compounds; Western Blots with BE(2)-C cells; Copies of ^{1}H- and ^{13}C-NMR-spectra of compound 4g.

This material is available free of charge via the Internet at http://pubs.acs.org.

AUTHOR INFORMATION

Corresponding author: *Phone: +497612034896. E-mail: manfred.jung@pharmazie.uni-freiburg.de

ACKNOWLEDGMENT

This work has been funded by the Deutsche Forschungsgemeinschaft (HDAC6: Ju295/10-2 within CRU201; HDAC8: Ju295/13-1, Si846/13-1, OE542/2-1 and WI1461/4-1, acetylation in leukemia: Ju295/9-2 within SPP1463). The work of CR and MM was supported by institutional funds from the Centre National de la Recherche Scientifique (CNRS), the Institute National de la Santé et de la Recherche Médicale (INSERM), the Université de Strasbourg, the French Infrastructure for Integrated Structural Biology (FRISBI) ANR-10-INSB-05-01 and Instruct as part of the European Strategy Forum on Research Infrastructures (ESFRI).

ABBREVIATIONS

Ac, acetyl; AMC, aminomethylcoumarin; APCI, atmospheric pressure chemical ionization; ATCC, American Type Culture Collection; DMEM, Dulbecco's modified Eagle's medium; ESI electrospray ionization; FBS, fetal bovine serum; GAPDH, glyceraldehyde 3-phosphate dehydrogenase; GI_{50}, half maximal growth inhibition; H3, histone 3; HA, heavy atom; HAT, histone acetyl transferase; HRP, horse radish peroxidase; LE, ligand efficiency; MeCN, Acetonitrile; MTS, 3-(4,5-dimethylthiazol-2-yl)-5-(3-carboxymethoxyphenyl)-2-(4-sulfophenyl)-2H-tetrazolium; *N*-MM, *N*-methylmorpholine; PMS, phenazine methosulfate; SDS-PAGE, sodium dodecyl sulfate polyacrylamide gel electrophoresis; TBS-T, Tris-buffered saline with 0.1% Tween 20; SF, selecitvity factor; ZMAL, (S)-[5-Acetylamino-1-(4-methyl-2-oxo-2H-chromen-7-ylcarbamoyl)-pentyl]-carbamic acid benzyl ester; *Z*, benzyloxycarbonyl.

REFERENCES

1. Dallavalle, S.; Pisano, C.; Zunino, F. Development and therapeutic impact of HDAC6-selective inhibitors. *Biochem. Pharmacol.* **2012,** *84* (6), 756-765.

2. Matsuyama, A.; Shimazu, T.; Sumida, Y.; Saito, A.; Yoshimatsu, Y.; Seigneurin-Berny, D.; Osada, H.; Komatsu, Y.; Nishino, N.; Khochbin, S.; Horinouchi, S.; Yoshida, M. In vivo destabilization of dynamic microtubules by HDAC6-mediated deacetylation. *EMBO J.* **2002,** *21* (24), 6820-6831.

3. Zuo, Q.; Wu, W.; Li, X.; Zhao, L.; Chen, W., HDAC6 and SIRT2 promote bladder cancer cell migration and invasion by targeting cortactin. *Oncol. Rep.* **2012,** *27* (3), 819-824.

4. Bali, P.; Pranpat, M.; Bradner, J.; Balasis, M.; Fiskus, W.; Guo, F.; Rocha, K.; Kumaraswamy, S.; Boyapalle, S.; Atadja, P.; Seto, E.; Bhalla, K. Inhibition of histone deacetylase 6 acetylates and disrupts the chaperone function of heat shock protein 90: a novel basis for antileukemia activity of histone deacetylase inhibitors. *J. Biol. Chem.* **2005,** *280* (29), 26729-26734.

5. Kalin, J. H.; Bergman, J. A., Development and therapeutic implications of selective histone deacetylase 6 inhibitors. *J. Med. Chem.* **2013,** *56* (16), 6297-6313.

6. Hubbert, C.; Guardiola, A.; Shao, R.; Kawaguchi, Y.; Ito, A.; Nixon, A.; Yoshida, M.; Wang, X. F.; Yao, T. P. HDAC6 is a microtubule-associated deacetylase. *Nature* **2002,** *417* (6887), 455-458.

7. Gao, L.; Cueto, M. A.; Asselbergs, F.; Atadja, P. Cloning and functional characterization of HDAC11, a novel member of the human histone deacetylase family. *J. Biol. Chem.* **2002,** *277* (28), 25748-25755.

8. Grozinger, C. M.; Hassig, C. A.; Schreiber, S. L. Three proteins define a class of human histone deacetylases related to yeast Hda1p. *Proc. Natl. Acad. Sci. U. S. A.* **1999,** *96* (9), 4868-4873.

9. Hideshima, T.; Bradner, J. E.; Chauhan, D.; Anderson, K. C. Intracellular protein degradation and its therapeutic implications. *Clin. Cancer Res.* **2005,** *11* (24 Pt 1), 8530-8533.

10. Li, Y. S., D.; Kwon, S. H. Histone deacetylase 6 plays a role as a distinct regulator of diverse cellular processes. *FEBS J.* **2013,** *280* (3), 775-793.

11. Zhang, Y.; Kwon, S.; Yamaguchi, T.; Cubizolles, F.; Rousseaux, S.; Kneissel, M.; Cao, C.; Li, N.; Cheng, H. L.; Chua, K.; Lombard, D.; Mizeracki, A.; Matthias, G.; Alt, F. W.; Khochbin, S.; Matthias, P. Mice lacking histone deacetylase 6 have hyperacetylated tubulin but are viable and develop normally. *Mol. Cell Biol.* **2008,** *28* (5), 1688-1701.

12. Govindarajan, N.; Rao, P.; Burkhardt, S.; Sananbenesi, F.; Schluter, O. M.; Bradke, F.; Lu, J.; Fischer, A. Reducing HDAC6 ameliorates cognitive deficits in a mouse model for Alzheimer's disease. *EMBO Mol. Med.* **2013,** *5* (1), 52-63.

13. Iwata, A.; Riley, B. E.; Johnston, J. A.; Kopito, R. R. HDAC6 and microtubules are required for autophagic degradation of aggregated huntingtin. *J. Biol. Chem.* **2005,** *280* (48), 40282-40292.

14. Dompierre, J. P.; Godin, J. D.; Charrin, B. C.; Cordelieres, F. P.; King, S. J.; Humbert, S.; Saudou, F. Histone deacetylase 6 inhibition compensates for the transport deficit in Huntington's disease by increasing tubulin acetylation. *J. Neurosci.* **2007,** *27* (13), 3571-3583.

15. Kawaguchi, Y.; Kovacs, J. J.; McLaurin, A.; Vance, J. M.; Ito, A.; Yao, T. P. The deacetylase HDAC6 regulates aggresome formation and cell viability in response to misfolded protein stress. *Cell* **2003,** *115* (6), 727-738.

16. Aldana-Masangkay, G. I.; Sakamoto, K. M. The role of HDAC6 in cancer. *J. Biomed. Biotechnol.* **2011,** *2011*, 875824.

17. Mergen, M.; Engel, C.; Muller, B.; Follo, M.; Schafer, T.; Jung, M.; Walz, G. The nephronophthisis gene product NPHP2/Inversin interacts with Aurora A and interferes with HDAC6-mediated cilia disassembly. *Nephrol. Dial. Transplant.* **2013,** *28* (11), 2744-2753.

18. Haggarty, S. J.; Koeller, K. M.; Wong, J. C.; Grozinger, C. M.; Schreiber, S. L. Domain-selective small-molecule inhibitor of histone deacetylase 6 (HDAC6)-mediated tubulin deacetylation. *Proc. Natl. Acad. Sci. U. S. A.* **2003,** *100* (8), 4389-4394.

19. Ai, T.; Xu, Y.; Qiu, L.; Geraghty, R. J.; Chen, L. Hydroxamic acids block replication of hepatitis C virus. *J. Med. Chem.* **2015,** *58* (2), 785-800.

20. Butler, K. V.; Kalin, J.; Brochier, C.; Vistoli, G.; Langley, B.; Kozikowski, A. P. Rational design and simple chemistry yield a superior, neuroprotective HDAC6 inhibitor, tubastatin A. *J. Am. Chem. Soc.* **2010,** *132* (31), 10842-10846.

21. Vishwakarma, S.; Iyer, L. R.; Muley, M.; Singh, P. K.; Shastry, A.; Saxena, A.; Kulathingal, J.; Vijaykanth, G.; Raghul, J.; Rajesh, N.; Rathinasamy, S.; Kachhadia, V.; Kilambi,

N.; Rajgopal, S.; Balasubramanian, G.; Narayanan, S. Tubastatin, a selective histone deacetylase 6 inhibitor shows anti-inflammatory and anti-rheumatic effects. *Int. Immunopharmacol.* **2013,** *16* (1), 72-78.

22. Santo, L.; Hideshima, T.; Kung, A. L.; Tseng, J. C.; Tamang, D.; Yang, M.; Jarpe, M.; van Duzer, J. H.; Mazitschek, R.; Ogier, W. C.; Cirstea, D.; Rodig, S.; Eda, H.; Scullen, T.; Canavese, M.; Bradner, J.; Anderson, K. C.; Jones, S. S.; Raje, N. Preclinical activity, pharmacodynamic, and pharmacokinetic properties of a selective HDAC6 inhibitor, ACY-1215, in combination with bortezomib in multiple myeloma. *Blood* **2012,** *119* (11), 2579-2589.

23. Schafer, S.; Saunders, L.; Eliseeva, E.; Velena, A.; Jung, M.; Schwienhorst, A.; Strasser, A.; Dickmanns, A.; Ficner, R.; Schlimme, S.; Sippl, W.; Verdin, E.; Jung, M. Phenylalanine-containing hydroxamic acids as selective inhibitors of class IIb histone deacetylases (HDACs). *Bioorg. Med. Chem.* **2008,** *16* (4), 2011-2033.

24. Schafer, S.; Saunders, L.; Schlimme, S.; Valkov, V.; Wagner, J. M.; Kratz, F.; Sippl, W.; Verdin, E.; Jung, M. Pyridylalanine-containing hydroxamic acids as selective HDAC6 inhibitors. *ChemMedChem* **2009,** *4* (2), 283-290.

25. Bergman, J. A.; Woan, K.; Perez-Villarroel, P.; Villagra, A.; Sotomayor, E. M.; Kozikowski, A. P. Selective histone deacetylase 6 inhibitors bearing substituted urea linkers inhibit melanoma cell growth. *J. Med. Chem.* **2012,** *55* (22), 9891-9899.

26. Jochems, J.; Boulden, J.; Lee, B. G.; Blendy, J. A.; Jarpe, M.; Mazitschek, R.; Van Duzer, J. H.; Jones, S.; Berton, O. Antidepressant-like properties of novel HDAC6-selective inhibitors with improved brain bioavailability. *Neuropsychopharmacol.* **2014,** *39* (2), 389-400.

27. Wagner, F. F.; Olson, D. E.; Gale, J. P.; Kaya, T.; Weiwer, M.; Aidoud, N.; Thomas, M.; Davoine, E. L.; Lemercier, B. C.; Zhang, Y. L.; Holson, E. B. Potent and selective inhibition of histone deacetylase 6 (HDAC6) does not require a surface-binding motif. *J. Med. Chem.* **2013,** *56* (4), 1772-1776.

28. Schlimme, S.; Hauser, A. T.; Carafa, V.; Heinke, R.; Kannan, S.; Stolfa, D. A.; Cellamare, S.; Carotti, A.; Altucci, L.; Jung, M.; Sippl, W. Carbamate prodrug concept for hydroxamate HDAC inhibitors. *ChemMedChem* **2011,** *6* (7), 1193-1198.

29. Sekar Reddy, A.; Suresh Kumar, M.; Ravindra Reddy, G. A convenient method for the preparation of hydroxamic acids. *Tetrahedron Lett.* **2000,** *41*, 6285-6288.

30. Ritson, D. J.; Spiteri, C.; Moses, J. E. A silver-mediated one-step synthesis of oxazoles. *J. Org. Chem.* **2011,** *76* (9), 3519-3522.

31. Huguet, F.; Melet, A.; Alves de Sousa, R.; Lieutaud, A.; Chevalier, J.; Maigre, L.; Deschamps, P.; Tomas, A.; Leulliot, N.; Pages, J. M.; Artaud, I. Hydroxamic acids as potent inhibitors of Fe(II) and Mn(II) E. coli methionine aminopeptidase: biological activities and X-ray structures of oxazole hydroxamate-EcMetAP-Mn complexes. *ChemMedChem* **2012,** *7* (6), 1020-1030.

32. Heltweg, B.; Trapp, J.; Jung, M. In vitro assays for the determination of histone deacetylase activity. *Methods* **2005,** *36* (4), 332-337.

33. Finnin, M. S.; Donigian, J. R.; Cohen, A.; Richon, V. M.; Rifkind, R. A.; Marks, P. A.; Breslow, R.; Pavletich, N. P. Structures of a histone deacetylase homologue bound to the TSA and SAHA inhibitors. *Nature* **1999,** *401* (6749), 188-193.

34. Hopkins, A. L.; Groom, C. R.; Alex, A. Ligand efficiency: a useful metric for lead selection. *Drug Discov. Today* **2004,** *9* (10), 430-431.

35. Hackanson, B.; Rimmele, L.; Benkisser, M.; Abdelkarim, M.; Fliegauf, M.; Jung, M.; Lubbert, M. HDAC6 as a target for antileukemic drugs in acute myeloid leukemia. *Leuk. Res.* **2012,** *36* (8), 1055-1062.

36. Heltweg, B.; Dequiedt, F.; Verdin, E.; Jung, M. Nonisotopic substrate for assaying both human zinc and NAD+-dependent histone deacetylases. *Anal. Biochem.* **2003,** *319* (1), 42-48.

37. Marek, M.; Kannan, S.; Hauser, A. T.; Moraes Mourao, M.; Caby, S.; Cura, V.; Stolfa, D. A.; Schmidtkunz, K.; Lancelot, J.; Andrade, L.; Renaud, J. P.; Oliveira, G.; Sippl, W.; Jung, M.; Cavarelli, J.; Pierce, R. J.; Romier, C. Structural basis for the inhibition of histone deacetylase 8 (HDAC8), a key epigenetic player in the blood fluke Schistosoma mansoni. *PLoS Pathog.* **2013,** *9* (9), e1003645.

38. UniProt, C., Activities at the Universal Protein Resource (UniProt). *Nucleic Acids Res* **2014,** *42* (Database issue), D191-198.

39. Bernstein, F. C.; Koetzle, T. F.; Williams, G. J.; Meyer, E. F., Jr.; Brice, M. D.; Rodgers, J. R.; Kennard, O.; Shimanouchi, T.; Tasumi, M. The Protein Data Bank: a computer-based archival file for macromolecular structures. *J. Mol. Biol.* **1977,** *112* (3), 535-542.

40. Altschul, S. F.; Gish, W.; Miller, W.; Myers, E. W.; Lipman, D. J. Basic local alignment search tool. *J. Mol. Biol.* **1990,** *215* (3), 403-410.

41. Sievers, F.; Wilm, A.; Dineen, D.; Gibson, T. J.; Karplus, K.; Li, W.; Lopez, R.; McWilliam, H.; Remmert, M.; Soding, J.; Thompson, J. D.; Higgins, D. G. Fast, scalable

generation of high-quality protein multiple sequence alignments using Clustal Omega. *Mol. Syst. Biol.* **2011,** *7*, 539.

42. Eswar, N.; Webb, B.; Marti-Renom, M. A.; Madhusudhan, M. S.; Eramian, D.; Shen, M. Y.; Pieper, U.; Sali, A. Comparative protein structure modeling using Modeller. *Curr. Protoc. Bioinformatics* **2006,** *Chapter 5*, Unit 5 6.

43. Suite 2012: Maestro version 9.3, Protein Preparation Wizard, Epik version 2.3, Glide version 5.8, Schrödinger, LLC, New York, NY, **2012**.

44. Molecular Operating Environment (MOE) 2012.10; Chemical Computing Group Inc., 1010 Sherbooke St. West, Suite #910, Montreal, QC, Canada, H3A 2R7, **2012**.

Table of contents graphic (TOC)

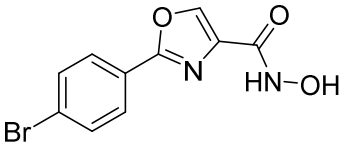

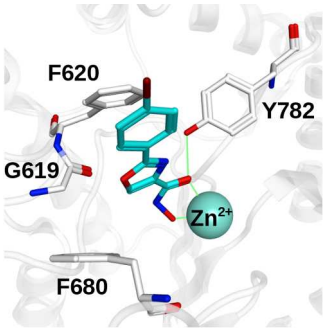

IC_{50} HDAC6: 59 nM
HDAC1: 14 μM
HDAC8: 14 μM